Published in final edited form as:
Biochemistry. 1996 May 7; 35(18): 5696–5704. doi:10.1021/bi953057k.

Cholesterol-Induced Interfacial Area Condensations of Galactosylceramides and Sphingomyelins with Identical Acyl Chains†

Janice M. Smaby, **Maureen Momsen**, **Vitthal S. Kulkarni**, and **Rhoderick E. Brown***
The Hormel Institute, University of Minnesota, 801 16th Avenue NE, Austin, Minnesota 55912

Abstract

The interfacial interactions occurring between cholesterol and either galactosylceramides (GalCers) or sphingomyelins (SMs) with identical acyl chains have been investigated using Langmuir film balance techniques. Included among the synthesized GalCers and SMs were species containing palmitoyl (16:0), stearoyl (18:0), oleoyl [18:$1^{\Delta 9(c)}$], nervonoyl [24:$1^{\Delta 15(c)}$], or linoleoyl [18:$2^{\Delta 9,12(c)}$] acyl residues. The cholesterol-induced condensations in the average molecular areas of the monolayers were determined by classic mean molecular area vs composition plots as well as by expressing the changes in terms of sphingolipid cross-sectional area reduction over the surface pressure range from 1 to 40 mN/m (at 1 mN/m intervals). The results show that, at surface pressures approximating bilayer conditions (30 mN/m), acyl heterogeneity in naturally occurring SMs (bovine or egg SM) enhanced the area condensation induced by cholesterol compared to their predominant molecular species (e.g. 18:0 SM in bovine SM; 16:0 SM in egg SM). Nonetheless, cholesterol always had a greater condensing effect on SM compared to GalCer when these sphingolipids were acyl chain matched and in similar phase states (prior to mixing with cholesterol). Also, the cholesterol-induced area changes for a given sphingolipid type (e.g. SM or GalCer) were similar whether the acyl chains were saturated, *cis*-Δ9-monounsaturated, or *cis*-Δ9,12-diunsaturated if the sphingolipids were in similar phase states (prior to mixing with cholesterol) and compared at equivalent surface pressures. These results indicate that, under conditions where hydrocarbon structure is matched, the sphingolipid head group plays a dominant role in determining the extent to which cholesterol reduces sphingolipid cross-sectional area. Despite the larger cholesterol-induced area condensations observed in SMs compared to those in GalCers, the molecular-packing densities showed that equimolar GalCer–cholesterol films were generally packed as tight as or slightly tighter than those of the SM–cholesterol films. The results are discussed in terms of a molecular model for sphingolipid–cholesterol interactions. Our findings also not only raise questions as to whether cholesterol-induced condensation data provide a reliable measure of the affinity, i.e. interaction strength, between cholesterol and different lipids but also provide insight regarding the stability of sterol/sphingolipid-rich microdomains thought to exist in caveolae and other cell membrane regions.

†This investigation was supported by USPHS Grant GM45928 (R.E.B.) and the Hormel Foundation. The automated Langmuir film balance used in this study receives major support from USPHS Grants HL49180 and HL17371 (H. L. Brockman, P. I.).

*Correspondence to Dr. Rhoderick E. Brown, The Hormel Institute, University of Minnesota, 801 16th Avenue NE, Austin, MN 55912. Fax: (507) 437-9606. reb@maroon.tc.umn.edu.

Interest in the in-plane interactions that occur between cholesterol and simple sphingolipids has been stimulated by recent discoveries in virology and cell biology. Semliki Forest virus requires cholesterol in target membranes for binding, but the fusion event is dependent upon simple sphingolipids such as sphingomyelin, ceramide, or galactosylceramide being present in target membranes (Nieva et al., 1994; Wilschut et al., 1995). Other envelope viruses, such as HIV,[1] are enriched in sphingomyelin and possess high cholesterol:phospholipid ratios compared to host cell plasma membranes (Aloia et al., 1993). With regard to the sorting of integral membrane proteins in the Golgi apparatus, the cholesterol–sphingolipid concentration is hypothesized to play a critical role in formation of membrane microdomains that differ in thickness from other regions. During sorting, Golgi proteins, but not plasma membrane proteins, may be excluded from the thicker, cholesterol-rich microdomains due to dimensional and compositional differences in their transmembrane helices (Bretscher & Munro, 1993). The trafficking, sorting, and localization of proteins bearing covalently attached glycosylphosphatidylinositol (GPI) lipid anchors also has been linked to specialized membrane regions enriched in cholesterol, glycosylceramides, and sphingomyelin [for recent review, see Parton and Simons (1995)]. Determining and verifying the molecular details of these interesting cell biological processes requires that the nature of the in-plane interactions between cholesterol and simple sphingolipids be clearly defined.

An effective way to investigate the in-plane interactions between cholesterol and other lipids is by Langmuir film balance approaches [e.g. Phillips (1972)]. An important advantage of studying lipid–lipid interactions using the monolayer approach is that the range of molecular areas known to occur in membrane systems can be investigated systematically while avoiding the mesomorphic changes that often occur in bulk hydrated dispersions (e.g. bilayer vesicles) as lipid composition is varied. Also, the in-plane lipid–lipid interactions can be isolated from the influences of changing transbilayer compositional distributions that may occur in bilayer systems when cholesterol mole fractions are varied [e.g. Sankaram and Thompson (1991) and Harris et al. (1995)]. For these reasons, monolayer investigations of sphingolipid–cholesterol interactions have proven useful (Lund-Katz et al., 1988; Johnston & Chapman, 1988; Grönberg et al., 1991; Slotte et al., 1993; Ali et al., 1994; Smaby et al., 1994; Bittman et al., 1994). In these earlier studies, interactions between cholesterol and different sphingolipids were evaluated by directly measuring the average cross-sectional molecular areas at various mixing ratios and surface pressures. The extent to which the average molecular area in a mixed composition film decreased below that predicted by summing the known molecular areas of the pure lipids (apportioned by mole fraction) provided a measure of the area condensation induced by cholesterol. This classic monolayer approach originally was used to show the marked condensing effect that cholesterol has on fluid-phase phosphoglycerides [e.g. Phillips, (1972) and references therein]. As a result, the extent of lipid monolayer condensation induced by cholesterol sometimes has been used as

[1]Abbreviations: GalCer, galactosylceramide; SM, sphingomyelin; HIV, human immunodeficiency virus; GPI, glycosylphosphatidylinositol; 16:0 GalCer, *N*-16:0 galactosylsphingosine; 18:0 GalCer, *N*-18:0 galactosylsphingosine; 18:1 GalCer, *N*-18:1$^{\Delta 9(c)}$galactosylsphingosine; 18:2 GalCer, *N*-18:2$^{\Delta 9,12(c)}$galactosylsphingosine; 24:1 GalCer, *N*-24:1$^{\Delta 15(c)}$galactosylsphingosine; 16:0 SM, *N*-16:0 sphingosylphosphocholine; 18:0 SM, *N*-18:0 sphingosylphosphocholine; 18:1 SM, *N*-18:1$^{\Delta 9(c)}$sphingosylphosphocholine; 18:2 SM, *N*-18:2$^{\Delta 9,12(c)}$sphingosylphosphocholine; 24:1 SM, *N*-24:1$^{\Delta 15(c)}$ sphingosylphosphocholine; PC, diacyl-*sn*-glycero-3-phosphocholine; PE, diacyl-*sn*-glycero-3-phosphoethanolamine; PA, diacyl-*sn*-glycero-3-phosphate.

an indicator of affinity or interaction strength that cholesterol has for various phosphoglycerides or sphingolipids [e.g. de Kruyff et al., (1973), Lund-Katz et al. (1988), Grönberg et al. (1991), and Slotte et al. (1993)].

Using the area condensation approach, Johnston and Chapman (1988) and Slotte et al. (1993) investigated the mixing behavior of cholesterol with galactosylceramides (GalCer) containing their naturally occurring, mixed complement of acyl chains. Slotte et al. (1993) concluded that GalCer does not interact with cholesterol because no area condensation was observed. Subsequently, we showed that significant molecular area condensation does occur when cholesterol is mixed with GalCer if the acyl composition imparts fluid-phase behavior to this sphingolipid prior to mixing with cholesterol (Ali et al., 1994). Even when the acyl structure of GalCer was modified so as to maximize area condensation upon mixing with cholesterol, larger effects were observed with egg or bovine brain sphingomyelin (SM) than with GalCer when these sphingolipids were in comparable phase states prior to mixing with cholesterol (Ali et al., 1994).

Recently, we noted that the acyl chain heterogeneity of egg and bovine brain SM significantly broadened the surface pressure range of their phase transitions compared to those of their predominant molecular species (e.g. egg SM = 86% 16:0 SM; bovine brain SM = 63% 18:0 SM) (Smaby et al., 1996). An examination of earlier studies, in which the cholesterol-induced condensations of SMs and other lipids had been compared, revealed that phase transitional broadening was probably an unrecognized contributor that enhanced the area condensations of SM. Here, we have synthesized different GalCer and SM species containing identical acyl chains (e.g. oleate, nervonate, and linoleate) as well as the predominant acyl residues in egg SM (palmitate) and in bovine SM (stearate). We have investigated the mixing behavior of these sphingolipids and cholesterol with two aims in mind: (1) to assess the contribution of phase transitional broadening to the cholesterol-induced condensations of naturally occurring SMs and (2) to carefully compare not only the changes in SM and GalCer cross-sectional area induced by cholesterol but also the effect that the sterol has on the molecular interfacial-packing density of GalCer relative to that of SM.

MATERIALS AND METHODS

Cholesterol was obtained from NuChek Prep (Elysian, MN). Egg and bovine brain SM were purchased from Avanti Polar Lipids (Alabaster, AL), and psychosine was obtained from Matreya, Inc. (Pleasant Gap, PA). GalCers and SMs containing homogeneous acyl chains were synthesized by reacylating psychosine and sphingosylphosphocholine, respectively, with the *N*-hydroxysuccinimide ester of the desired fatty acid (Kulkarni et al., 1995; Smaby et al., 1996). No dihydropsychosine was evident by thin layer chromatography TLC). After purification by flash chromatography and recrystallization, all lipids were greater than 99% pure on the basis of TLC analysis. Acyl homogeneity of the semisynthetic GalCer and SM derivatives was confirmed by quantitatively releasing, methylating, and analyzing the fatty acyl residues via capillary gas chromatography (Smaby et al., 1996). The acyl composition of egg SM consisted of 86% palmitate (16:0), 0.4% myristate, 4.8% stearate (18:0), 1.1% arachidate (20:0), 2.5% behenate (22:0), 1.0% lignocerate (24:0), and 4.2% nervonate

(24:1$^{\Delta 15}$). Bovine brain SM's acyl composition consisted of 63% stearate (18:0), 2.4% palmitate (16:0), 6.6% arachidate (20:0), 9.2% behenate (22:0), 6.1% lignocerate (24:0), and 13% nervonate (24:1$^{\Delta 15}$). Stock solutions were prepared by dissolving lipids in either petroleum ether–ethanol (95:5), hexane (Burdick Jackson Lab., Muskegon, MI)–ethanol (95:5), or hexane–2-propanol–water (70:30:2.5). Solvent purity was verified by surface potential measurements (Smaby & Brockman, 1991). SMs were quantitated by phosphate assay (Bartlett, 1959). GalCers and cholesterol were quantitated gravimetrically. GalCer stock concentrations also were confirmed by capillary gas chromatography using 17:0 SM as an internal standard. This proved to be more reliable than the Sloan–Stanley assay for nitrogen content which we used previously [e.g. Ali et al. (1994)]. Water for the subphase buffer was purified by reverse osmosis, mixed-bed deionization, adsorption on activated charcoal, and filtration through a 0.22 μm Durapore membrane (Millipore Corp., Bedford, MA). Subphase buffer consisted of 10 mM potassium phosphate, 100 mM NaCl, and 0.2% sodium azide at a pH of 6.6. Buffer was filtered through a Diaflo hollow fiber filter with a molecular weight cutoff of 10 000 (Amicon Corp., Danvers, MA) and stored under argon until use.

Monolayer Studies

A computer-controlled, Langmuir-type film balance, calibrated according to the equilibrium-spreading pressures of known lipid standards (Smaby & Brockman, 1990) and housed in a laboratory with a filtered air supply, was used to measure the surface pressure vs molecular area ($\pi - A$) of the lipid mixtures. Prior to use, glassware was acid cleaned and then rinsed thoroughly with deionized water and hexane–ethanol (95:5). Lipids were spread in 51.7 μL solvent aliquots onto a trough filled with ~845 mL of phosphate–saline buffer (pH 6.6). Film compression was initialized after a 4 min delay and proceeded at a rate of ≤4 Å^2 molecule^{-1} min^{-1}. The subphase temperature was kept at 24 ± 1 °C by a temperature-controlled water bath. Surface potential was measured using a ^{210}Po ionizing electrode.

Analysis of Isotherms

Mixing behavior in two-component lipid monolayers was analyzed by mean molecular area–composition diagrams (Ali et al., 1994; Smaby et al., 1994). Experimentally observed areas in the mixtures were compared with areas calculated by summing the molecular areas of the pure components (apportioned by mole fraction in the mix). The calculated, mean molecular areas (A_π) of two-component mixtures were determined at a given surface pressure (π) using the following equation:

$$A_\pi = X_1(A_1)_\pi + (1 - X_1)(A_2)_\pi \quad (1)$$

where X_1 is the mole fraction of component 1 and $(A_1)_\pi$ and $(A_2)_\pi$ are the mean molecular areas of pure components 1 and 2 at identical surface pressures. Negative deviations from additivity indicated condensation and implied intermolecular accommodation and/or dehydration interactions between lipids in the mixed films [e.g. Cadenhead and Müller-Landau (1980)].

The cholesterol-induced condensation, i.e. cross-sectional area reduction, of the sphingolipid (SL) molecules was calculated at constant surface pressure as follows:

$$\text{SL condensation} = A_{\text{SL}} - [A_{\text{mix}} - (A_{\text{chol}} X_{\text{chol}})]/X_{\text{SL}} \quad (2)$$

where SL condensation units are squared angstroms per SL molecule, A_{SL} is the area per molecule of the pure sphingolipid, A_{mix} is the average area per molecule of the SL–chol mixed monolayer, A_{chol} is the area per molecule of the pure cholesterol, X_{chol} is the mole fraction of cholesterol in the mixed monolayer, and X_{SL} is the mole fraction of sphingolipid in the mixed film. Calculating the area reduction in terms of SL condensation is valid because the surface area of cholesterol changes very little with increasing surface pressure (Phillips, 1972). We determined the cross-sectional areas of pure cholesterol to be 37.6, 37.2, and 36.8 $Å^2$ at surface pressures of 5, 15, and 30 mN/m (Ali et al., 1994).

RESULTS

Does Phase Transitional Broadening Influence the Cholesterol-Induced Area Condensations in SMs?

To address this issue, we investigated mixtures of 16:0 SM–cholesterol and of 18:0 SM–cholesterol and compared the results with our earlier egg SM–cholesterol and bovine brain SM–cholesterol data (Smaby et al., 1994). Figure 1 shows the effect of increasing cholesterol content on the surface pressure vs *apparent* molecular area ($\pi - A$) of 16:0 SM (Figure 1D) and of 18:0 SM (Figure 1B). The sphingolipid *apparent* molecular area was calculated by dividing the total surface area of the cholesterol–phingolipid mixed monolayers by the number of sphingolipid molecules applied to the surface. Expressing the $\pi - A$ data in this manner permitted identical area scales (abscissas) to be used and facilitated viewing, especially in mixtures where the $\pi - A$ behavior of the pure components differed by only a few square angstroms per molecule [e.g. 18:0 GalCer and cholesterol (Figure 1A); 16:0 GalCer and cholesterol (Figure 1C)]. In Figure 1, the effect of increasing cholesterol on the two-dimensional phase transitions in 18:0 SM (Figure 1B) and in 16:0 SM (Figure 1D) is clearly evident. At low cholesterol mole fractions (<0.2), the transitions are visible but then disappear at higher sterol mole fractions. The overlapping portions of the isotherms in the 18:0 SM and 16:0 SM series indicate a large condensing effect by cholesterol.

To quantitate the cholesterol condensing effect, we analyzed the additivity of the mean molecular areas vs cholesterol content (see Materials and Methods). Figure 3 shows the results at three different surface pressures (5, 15, and 30 mN/m) for 16:0 SM (panel D) and 18:0 SM (panel B). Solid lines represent ideal additivity. The corresponding data for egg SM and bovine SM are shown in Figure 3C and Figure 4A of Smaby et al. (1994). Negative deviations from additivity were most prominent at surface pressures resulting in liquid-expanded, i.e. chain-disordered, behavior in the absence of cholesterol. This behavior was evident in 18:0 SM at 5 mN/m and in 16:0 SM at both 5 and 15 mN/m. The negative deviations from additivity for 18:0 SM and for 16:0 SM remained relatively large until increasing surface pressure induced transitions to chain-ordered, liquid-condensed states (Figure 3B,D). This transition began near 7 mN/m and ended near 17 mN/m for 18:0 SM

and began near 20 mN/m and ended near 30 mN/m for 16:0 SM (Smaby et al., 1996). At high surface pressures where 18:0 and 16:0 SM were in chain-ordered states, the area condensation induced by cholesterol was strongly mitigated (Figure 3; panels B,D, 30 mN/m).

The mean molecular area vs composition plots show that the average molecular area reduction that occurs with increasing cholesterol results not only because the cross-sectional area of the sterol (37 ± 0.5 $Å^2$/molecule) is smaller than that of chain-disordered, fluid-phase SMs but also because favorable accommodation interactions occur in the mixed films (negative deviations from additivity). In fact, the favorable accommodation, i.e. condensation, must be due to cross-sectional area changes that occur almost exclusively in SM because cholesterol is a rigid, relatively inflexible molecule with a cross-sectional area that varies little with increasing surface pressure [e.g. Phillips (1972)]. To focus on the condensation event and compare our data with earlier results expressed in a similar manner (Lund-Katz et al., 1988; Smaby et al., 1994), we calculated the area reductions in terms of sphingolipid molecular area condensation (see Materials and Methods; eq 2). Figure 5 shows the sphingolipid area condensation as a function of increasing surface pressure at equimolar cholesterol. Expressing the data in this way illustrates how both surface pressure and sphingolipid phase state influence the magnitude of cholesterol-induced condensation. The results in Figure 5 not only verified the conclusions drawn from the classic mean molecular area vs composition plots (Figure 3B) but also provided intriguing new insights into the cholesterol–SM interaction. For instance (from Figure 5), it is clear that the cholesterol-induced area condensations of egg SM and of bovine brain SM remained higher than those of 16:0 SM and of 18:0 SM at high surface pressures (π > 25 mN/m). In fact, at 30 mN/m, values were nearly twice as high for egg SM and for bovine brain SM as for 16:0 SM and for 18:0 SM (10 vs 5 $Å^2$/molecule).

Does Cholesterol Induce Greater Area Condensation of SMs Compared to Those of GalCers?

Although we had previously compared the cholesterol-induced area condensations of egg or bovine brain SM with those of various GalCers (Ali et al., 1994), reassessment was warranted due to the diminished sterol-induced condensations observed with 16:0 SM or 18:0 SM compared to that observed for egg SM or bovine SM, respectively. To accomplish this, we synthesized SMs and GalCers that were acyl chain-matched to avoid the problems caused by chain heterogeneity. These included not only 16:0 GalCer and 18:0 GalCer but also the oleoyl (18:1), nervonoyl (24:1), and linoleoyl (18:2) derivatives of GalCer and SM. The effects of increasing cholesterol on the $\pi - A$ isotherms of the acyl chain-matched SMs and GalCers are shown in Figures 1 and 2.

The isotherms in Figure 1 show that increasing cholesterol has very similar effects on 18:0 GalCer (Figure 1A) and 16:0 GalCer (Figure 1C). The isotherms are distinctly different from those of 18:0 SM (Figure 1B) and 16:0 SM (Figure 1D) which show two-dimensional phase transitions at low sterol mole fractions. Interestingly, introducing monounsaturated acyl chains into the sphingolipids produced marked changes in their behavior and in their mixing response with cholesterol. The $\pi - A$ data for both 18:1 GalCer–cholesterol (Figure

2A) and 18:1 SM–cholesterol (Figure 2B) show that these sphingolipids are chain-disordered at all surface pressures below film collapse and that increasing cholesterol condenses the films. In contrast, 24:1 GalCer (Figure 2C) and 24:1 SM (Figure 2D) both showed phase transitions as pure compounds and at low cholesterol mole fractions despite the presence of the acyl chain *cis* double bond. The transitions in 24:1 GalCer were atypical in that pronounced metastability was evident, a feature previously noted in 24:1 GalCer and in naturally occurring fractions containing 24:1 GalCer (Johnston & Chapman, 1988; Ali et al., 1994). In the case of 24:1 SM, the subtle phase transition beginning near 30 mN/m also was demonstrated by recent elastic area compressibility moduli measurements (Smaby et al., 1996). The behavior of these monounsaturated sphingolipid species (18:1 and 24:1) was of interest due to their natural occurrence, not only in bovine brain, but also in human aorta and optic lens fiber cells and in egg yolk.

From the surface pressure vs apparent molecular area data measured at increasing mole fractions of cholesterol (Figures 1 and 2), we quantitated the cholesterol-induced area condensation using mean molecular area vs composition plots for the chain-matched GalCer and SM derivatives (Figures 3 and 4). Minimal deviations from additivity were observed at all surface pressures between 1 and 40 mN/m for 18:0 and 16:0 GalCer because these lipids were already highly ordered (liquid-condensed) prior to mixing with cholesterol (Figure 3A,C). In contrast, relatively large area negative deviations from additivity were observed for 18:1 GalCer and SM at 5, 15, and 30 mN/m because these derivatives were liquid-expanded and in chain-disordered states in the absence of cholesterol (Figure 4A,B). Similar behavior was observed with 18:2 GalCer and 18:2 SM (data not shown).

The negative deviations from additivity for 24:1 GalCer and 24:1 SM remained relatively large only until increasing surface pressures induced transitions to chain-ordered, liquid-condensed states (Figure 2C,D). Because this transition occurs near 8 mN/m for 24:1 GalCer (Figure 2C), only the 5 mN/m but not the 15 or 30 mN/m data in Figure 4C showed significant negative deviation from additivity. In contrast, because this transition occurs near 35 mN/m for 24:1 SM (Smaby et al., 1996), significant negative deviations from additivity were observed at 5, 15, and 30 mN/m (Figure 4D).

To focus on the condensation process, we calculated the area reductions in terms of sphingolipid molecular area condensation as described in Materials and Methods (eq 2). Figure 5 shows the results and permits easy comparison of the condensation values of chain-matched SMs and GalCers [e.g. 18:1 GalCer and 18:1 SM, 18:2 GalCer and 18:2 SM, or 24:1 GalCer and 24:1 SM (at $\pi < 10$ mN/m)]. At equivalent π (e.g. 5 or 30 mN/m), equimolar cholesterol consistently induced area reductions in the SMs that were 20–25% greater than those induced in the corresponding GalCers. A similar trend was observed regarding the condensation of chain-ordered, i.e. liquid-condensed, GalCers and SMs (e.g. 16:0 GalCer and 16:0 SM or 18:0 GalCer and 18:0 SM) by cholesterol. In this case, the SMs showed area condensations of about 5 $Å^2$/molecule at 30 mN/m, whereas the GalCers showed almost none (either 0 or 2 $Å^2$/molecule).

Interestingly, the data in Figure 5 also show that the magnitudes of the area changes induced by cholesterol were similar for a given sphingolipid type (e.g. SM or GalCer) regardless of

whether that sphingolipid contained saturated, *cis*-Δ9-monounsaturated, or *cis*-Δ9,12-diunsaturated acyl chains under conditions of equivalent phase state and surface pressure (prior to mixing with cholesterol). For instance, at 30 mN/m, similar levels of condensation were observed in 18:2 SM, 18:1 SM, or 24:1 SM as well as in 18:1 GalCer or 18:2 GalCer. When the surface pressure was low enough to yield liquid-expanded behavior in SMs with saturated acyl chains (e.g. 5 mN/m), then these SM species also displayed condensations similar to those of SMs that contained either monounsaturated or diunsaturated acyl chains.

What Effect Does Cholesterol Have on Sphingolipid-Packing Density?

While the data in Figure 5 do show clearly how both surface pressure and sphingolipid phase state affect the *change* in sphingolipid cross-sectional area brought about by cholesterol, this type of analysis provides no insight into the absolute sphingolipid surface-packing density before and after mixing with cholesterol. Figure 6 depicts the cross-sectional molecular areas of the various sphingolipids at 30 mN/m in the absence and presence of cholesterol. Data obtained at 30 mN/m were of particular interest because there is much evidence indicating that surface pressures in the 30–35 mN/m range approximate those found in each half of bilayer membranes (Phillips & Chapman, 1968; Demel et al., 1975; Evans & Waugh, 1977; Blume, 1979; Cevc & Marsh, 1987). In Figure 6, each horizontal line corresponds to a different sphingolipid derivative with GalCer derivatives having filled symbols and SMs having unfilled symbols at the ends of their lines. The right-hand symbol represents the cross-sectional molecular area of the pure lipid in the absence of cholesterol, whereas the left-hand symbol shows the condensed molecular area of each sphingolipid induced by either 0.5 (panel A) or 0.3 (panel B) mole fraction cholesterol. These latter values were calculated using eq 2 in Materials and Methods. The lengths of the horizontal lines connecting symbols represent the change in sphingolipid molecular area, i.e. condensation, produced upon mixing with cholesterol. Hence, the data in Figure 6 not only show the cholesterol-induced area condensations of various GalCer and SM species but also provide sphingolipid-packing densities before and after mixing with cholesterol.

Two conclusions were evident from the data in Figure 6. First, despite the lower area condensations induced in GalCer by cholesterol, the molecular-packing densities of GalCer–cholesterol films were quite similar or, in some cases, exceeded the packing densities achieved by SM–cholesterol films when the sphingolipids were matched with respect to acyl chain structure, phase state, and surface pressure prior to mixing with cholesterol. The data for 16:0 GalCer and SM, 18:0 GalCer and SM, 18:1 GalCer and SM, and 18:2 GalCer and SM clearly support this finding. Second, within a given sphingolipid class and at equivalent surface pressures, the magnitude of cholesterol-induced area condensation was similar for different molecular species even when the absolute molecular-packing densities differed substantially. The data for 18:2 SM and 18:1 SM or 18:2 GalCer and 18:1 GalCer illustrate this latter point.

DISCUSSION

Impact of Phase Transitional Broadening on Cholesterol's Ability to "Condense" Sphingolipids

Our results clearly show that the cholesterol-induced condensation values for egg SM and bovine SM at surface pressures exceeding 25 mN/m are significantly higher than those observed with 16:0 SM and 18:0 SM. The simplest explanation for these findings is that the presence of 24:1 SM, which represents 4.2% of egg SM and 13% of bovine brain SM, broadens their respective two-dimensional phase transitions and extends the liquid-expanded/condensed phase coexistence region to high pressures. In fact, the cholesterol-induced condensation of 24:1 SM is nearly double that of egg or bovine brain SM at 30 mN/m because the onset of the 24:1 SM transition does not occur until about 30 mN/m (Smaby et al., 1996). At surface pressures above 30 mN/m, the condensation values of 24:1 SM appear to converge toward those of egg and bovine brain SM.

Attributing the enhanced, cholesterol-induced area condensation in egg or bovine SM to the presence of the fluid-phase SM that coexists with gel-phase SM in the transition region is consistent with the known response of fluid- but not gel-phase lipids to mixing with cholesterol. This has been clearly demonstrated in glycerol-based and sphingoid-based lipids [e.g. Ali et al. (1994) and Smaby et al. (1994) and references therein]. However, the impact of phase transitional broadening on cholesterol-induced condensations of SMs has not been fully appreciated because the true extent of the unusually broad and relatively subtle phase transitions in naturally occurring SMs was not apparent until very recently (Smaby et al., 1996). In fact, in previous studies, egg SM and 16:0 SM were used interchangeably in studies of cholesterol-induced area condensations because their behavior was thought to be so similar [e.g. Lund-Katz et al. (1988) and Smaby et al. (1994)].

Cholesterol's Condensation of SMs and GalCers with Identical Acyl Chains

Our results indicate that cholesterol does induce larger average molecular area *changes* in SMs than in GalCers under conditions of equivalent surface pressure, cholesterol content, and acyl composition. This clarifies the results of earlier reports in which measurements sometimes were performed under conditions where phase transitional broadening enhanced the observed cholesterol-induced area condensation of the SMs [e.g. Lund-Katz et al. (1988) and Ali et al. (1994)]. Despite the fact that cholesterol induces larger changes in the areas of SMs compared to those of GalCers, it is clear that cholesterol can have a significant condensing effect on GalCers. This point has been the subject of controversy in other recent investigations. In two earlier studies in which the mean molecular areas of cholesterol–GalCer films were measured, the focus was on naturally derived GalCer fractions which have heterogeneous acyl compositions (Johnston & Chapman, 1988; Slotte et al., 1993). Conflicting results were reported for the GalCer subfraction containing nonhydroxy fatty acyl chains. In contrast to Johnston and Chapman (1988), Slotte et al. (1993) observed no cholesterol-induced area condensation, leading them to conclude that there was no interaction between cholesterol and GalCer. Subsequently, we showed that significant molecular area condensation does occur when cholesterol is mixed with GalCer if the acyl

composition imparts fluid-phase behavior to the sphingolipid prior to mixing with cholesterol (Ali et al., 1994). The results presented here confirm this latter finding.

It is important to note that, in the absence of cholesterol, SMs occupy larger cross-sectional molecular areas than GalCers when acyl chains are identical and when the lipids are compared at equivalent surface pressures in the liquid-expanded region of their isotherms (Smaby et al., 1996). This behavior probably reflects differences in head group orientation and/or hydration of these sphingolipids. The smaller less-hydrated head group of GalCer [e.g. Ruocco and Shipley (1983) and Sen and Hui (1988)] may extend approximately normal to the lamellar interface in fully hydrated bilayers and monolayers [e.g. Bunow and Levin (1980), Jarrell et al. (1992), and Ali et al. (1993)] in contrast to the orientation of the bulkier, more hydrated, phosphocholine head group in SM which is more parallel (within 30°) to the lamellar plane (Bruzik, 1988). This points to the polar head group as playing an important role in establishing the initial packing density of the sphingolipid films at a given surface pressure (prior to mixing with cholesterol). In fact, if this difference in initial packing density is eliminated by normalizing chain-matched SM and GalCer to equivalent molecular areas (rather than equivalent surface pressures), then nearly identical mean molecular areas are observed upon mixing with cholesterol (Figure 7). Interestingly, PCs with hydrocarbon structures that match SM or GalCer also display similar behavior.

This leads to the following model as to how the cholesterol condenses SMs and GalCers. The primary effect of incorporating cholesterol, with its rigid planar steroid ring, is reduction of *trans–gauche* isomerization about the carbon–carbon bonds in the liquid-disordered (liquid-expanded) acyl chains of GalCer and SM [e.g. Speyer et al. (1989) and Morrow et al. (1995)]. In doing so, transient acyl kinks, which enhance the molecular cross-sectional area in the hydrocarbon region proximal to the lipid interface, become diminished so that optimal van der Waals interactions can be achieved between the hydrocarbon chain(s) and the α surface of the steroid ring which is held near the interface by a 3-β hydroxyl group (McIntosh et al., 1992a; Vanderkooi, 1994) and may hydrogen bond with the amide group of the sphingolipid (Sankaram & Thompson, 1991; Bittman et al., 1994). Because the cross-sectional area of cholesterol undergoes almost no change in response to increasing surface pressure, the bulk of the condensing effect induced by cholesterol must be due to ordering that occurs in the sphingolipid hydrocarbon region. However, this does not adequately explain why small but reproducible area condensations also are observed with sphingolipids that are already chain-ordered by virtue of high surface pressure prior to mixing with cholesterol. Hence, it appears that a secondary effect of cholesterol incorporation may be a change in sphingolipid average orientation. This change need not be confined to the polar head group region as implied previously (Ali et al., 1994). A more plausible explanation is that cholesterol relaxes the long-axis molecular tilt that probably occurs in the chain-ordered states of pure SM and GalCer monolayers. The net effect of sphingolipid reorientation to a long-axis normal position (with respect to the lamellar interface) would be a slight decrease in cross-sectional molecular area. Moreover, because the cholesterol-induced condensations in chain-ordered SMs consistently exceed those of chain-ordered GalCers, the resulting orientational changes would have to be larger for SMs

than for GalCers when their acyl chains are identical. We believe these suggestions are reasonable when viewed within the context of existing data in related lipid mixtures.

Consider the following. Recent evidence indicates that long-axis molecular tilt occurs in chain-ordered, gel state SM bilayers with respect to the lamellar plane (McIntosh et al., 1992a). By tilting, these phosphocholine-containing lipids increase the effective cross-sectional area of the hydrocarbon region so that the nonpolar area matches the phosphocholine head group area. Long-axis molecular tilt of lipids is not restricted to bilayers or to lipids with phosphocholine head groups. Indeed, long-axis molecular tilt has been reported in monolayers of condensed-phase PC as well as PA and PE (Vaknin et al., 1991; Helm et al., 1987, 1991). In fact, the tilt angle in PC monolayers is sensitive to whether acyl chains are ether- or ester-linked (Brezesinski et al., 1995). So, it is reasonable to assume that long-axis molecular tilt occurs in monolayers of chain-ordered sphingolipids.

When incorporated into the sphingolipid lattice, cholesterol may act like a head group spacer molecule because its polar head group area is small compared to that of phosphocholine (or galactose) yet this sterol's nonpolar area (37 $Å^2$/molecule) is similar to that of a condensed two-hydrocarbon chain lipid (39 $Å^2$/molecule). As a result, the driving force favoring chain tilt would no longer be present. Because the galactose head group in GalCer is smaller and less hydrated than the phosphocholine head group in SM, the tendency of GalCer to tilt would be less than that of SM when their ceramide regions are matched. Hence, the incorporation of cholesterol probably has a bigger impact on SM than on GalCer. The end result would be similar molecular-packing densities for both SM and GalCer in the presence of cholesterol as well as larger cholesterol-induced area condensations for chain-ordered (liquid-condensed) SMs compared to those of GalCers. In fact, this is what we observe experimentally. Interestingly, the changes in cross-sectional area observed in PC monolayers resulting from the elimination of molecular tilt are approximately 6 $Å^2$/molecule at 30 mN/m (Brezesinski et al., 1995) which is consistent with the molecular condensation value that we observe with SM. Also, NMR studies have shown that cholesterol mole fractions of 0.3 or more enhance the mobility of PC head groups by acting as spacers that separate the phosphocholine head groups (Yeagle et al., 1975; Oldfield et al., 1978).

Aside from acting as a simple spacer molecule, cholesterol also may reorganize the interfacial water, leading to changes in the intra- and intermolecular dipole interactions near the head group/interface region of the sphingolipids. Such changes might include alterations in the hydrogen-bonding interactions thought to occur in chain-ordered SM (Bruzik, 1988; Sankaram & Thompson, 1991; Bittman et al., 1994). Interestingly, McIntosh et al. (1992b) reported that the presence of equimolar cholesterol in SM bilayers alters the hydration pressure relative to that of pure SM bilayers. These same researchers also have shown that the addition of equimolar cholesterol to egg PC bilayers reduces interbilayer separation and allows the phosphocholine head groups of apposing bilayers to interpenetrate at high pressures (McIntosh et al., 1989).

Are Comparisons of Area Condensations Reliable Indicators of the Interaction Affinity of Cholesterol for Different Lipids?

From our results (Figure 6), it is clear that mixing of equimolar cholesterol with SMs does not result in molecular-packing densities that exceed those of GalCers. The cross-sectional area of SM is greater to begin with, but both SM and GalCer are limited as to how small they can become when cholesterol is added. Since each of these sphingolipids has two hydrocarbon chains per molecule, the close-packing limit cannot be smaller than the cross-sectional area of two crystalline hydrocarbon chains (~8 $Å^2$/molecule). Hence, the apparent molecular area *changes* induced by cholesterol in SMs exceed those of GalCers. Interestingly, this is not the case for SMs and PCs which have identical phosphocholine head groups. When their hydrocarbon structural differences are minimized, very similar apparent molecular area *changes* are induced by cholesterol (Smaby et al., 1994). These findings lead us to question whether comparing cholesterol-induced condensations is a valid way to determine the affinity, i.e. interaction strength, of cholesterol for different membrane lipids as has sometimes been done in the past. Indeed, our evidence indicates that use of area condensation measurements in this manner can be misleading. Other factors such as the final packing density must also be considered to provide a complete picture of sterol–lipid interactions.

This is not to say that investigations of cholesterol-induced condensation of membrane lipids are without value. In fact, just the opposite is true. From the data in Figure 6, it is clear that all of the GalCer derivatives that are liquid-expanded (at 30 mN/m) in the absence of cholesterol (e.g. 18:1 GalCer and 18:2 GalCer) undergo fairly similar area condensations (10–1 $Å^2$/GalCer molecule) upon mixing with equimolar cholesterol. The same situation occurs for liquid-expanded SM derivatives (e.g. 18:1 SM, 18:2 SM, and 24:1 SM) except that the magnitudes of the apparent area reductions are larger (14–5 $Å^2$/SM molecule) than that observed with the GalCers.

It should be emphasized that, with respect to molecular area change induced by equimolar cholesterol, the relative lack of sensitivity displayed by GalCer or SM to the unsaturation level in their acyl chains is not a feature unique to sphingolipids. Similar results have been reported for PCs containing *sn*-1 saturated chains (e.g. 16:0, 18:1 PC or 16: 0, 20:4 PC) (Smaby et al., 1994). However, the magnitude of the cholesterol-induced condensation of PC decreases if both acyl chains are unsaturated (e.g. di-18:1 PC or di-20:4 PC). Hence, it is clear that the extent to which cholesterol can reduce the cross-sectional areas of sphingolipids and phospholipids is critically linked to what might otherwise seem to be subtle structural differences. Interestingly, recent molecular dynamics computer simulations indicate that cholesterol does produce more *trans* dihedrals in the *sn*-1 chain than in the *sn*-2 chain of dimyristoyl-PC (Robinson et al., 1995).

Physiological Implications

The special environment that cholesterol and sphingolipids provide in membranes is thought to play an important role in protein sorting and localization [e.g. Bretscher and Munro (1993) and Parton and Simons (1995)]. Our results show that cholesterol enhances the interfacial packing density in GalCer and SM. More importantly, the cholesterol-induced

packing densities attained with GalCers or SMs are higher than those attained in PCs when hydrocarbon structures are similar (Smaby et al., 1994). These differences in cholesterol-induced interfacial packing densities are further exacerbated when the structural motifs of the naturally prevalent lipid forms are compared. For GalCer and SM, saturated acyl chains are typical, whereas for PC, saturated *sn*-1 and unsaturated *sn*-2 chains are the norm. The physical characteristics of the different cholesterol-induced interfacial packing densities in sphingoid-based and glycerol-based membrane lipids remain to be clearly defined but are likely to be important in modulating (i) detergent insolubility, (ii) the subcellular localization of certain integral membrane proteins (Bretscher & Munro, 1993) and proteins bearing GPI–lipid anchors (Schroeder et al., 1994; Hanada et al., 1995), and (iii) the lateral distribution of complex gangliosides such as those known to associate with caveolae (Parton, 1994; Palestini et al., 1995). Given the tight packing density that occurs in sphingolipid–cholesterol films, the rapid release of cholesterol from caveolae into the medium (Fielding & Fielding, 1995) is likely to be mediated by specific binding/transport proteins (Murata et al., 1995) that can translocate between the Golgi apparatus and surface caveolae (Smart et al., 1994).

From a biophysical viewpoint, the involvement of SMs in sphingolipid–cholesterol-rich microdomains makes the situation even more intriguing because SMs are one of a few naturally occurring membrane lipids whose fluid–gel coexistence region encompasses mammalian physiological temperatures [for review, see Koynova and Caffrey (1995)]. Cholesterol could easily modulate the phase behavior of the SMs by altering the size and nature of the coexisting fluid–solid domains, a situation known to occur in model membranes [e.g. Sankaram and Thompson (1991), Hwang et al. (1995), and Slotte (1995)]. In a future paper, we will show how cholesterol affects the interfacial elastic interactions of SMs and GalCers in ways that are not evident from area condensation measurements.

Acknowledgments

We thank Howard Brockman for the use of the Langmuir film balance and for helpful comments regarding this report, Margot Cleary and Fred Phillips for assistance with the capillary GC analyses of lipid acyl compositions, and Kristi Hyland for synthesizing and purifying several of the sphingolipid derivatives.

References

Ali S, Smaby JM, Brown RE. Biochemistry. 1993; 32:11696–1703. [PubMed: 8218238]

Ali S, Smaby JM, Brockman HL, Brown RE. Biochemistry. 1994; 33:2900–2906. [PubMed: 8130203]

Aloia RC, Tian H, Jensen FC. Proc Natl Acad Sci USA. 1993; 90:5181–5185. [PubMed: 8389472]

Bartlett GR. J Biol Chem. 1959; 234:466–468. [PubMed: 13641241]

Bittman R, Kasireddy CR, Mattjus P, Slotte JP. Biochemistry. 1994; 33:11776–11781. [PubMed: 7918394]

Blume A. Biochim Biophys Acta. 1979; 557:32–44. [PubMed: 549642]

Bretscher MS, Munro S. Science. 1993; 261:1280–1281. [PubMed: 8362242]

Brezesinski G, Dietrich A, Struth B, Böhm C, Bouwman WG, Kjaer K, Möhwald H. Chem Phys Lipids. 1995; 76:145–157.

Bruzik KS. Biochim Biophys Acta. 1988; 939:316–326.

Bunow MR, Levin IW. Biophys J. 1980; 32:1007–1021. [PubMed: 7260307]

Cadenhead DA, Müller-Landau F. J Colloid Interface Sci. 1980; 78:269–270.

Cevc, G.; Marsh, D. Phospholipid Bilayers. Wiley-Interscience; New York: 1987. p. 347-361.

de Krujff B, Demel RA, Slotboom AJ, van Deneen LLM, Rosenthal AF. Biochim Biophys Acta. 1973; 307:1–19. [PubMed: 4711186]

Demel RA, Guerts von Kessel WSM, Zwaal RFA, Roelofson B, van Deenen LLM. Biochim Biophys Acta. 1975; 406:97–107. [PubMed: 1174576]

Evans E, Waugh R. J Colloid Interface Sci. 1977; 60:286–298.

Fielding PE, Fielding CJ. Biochemistry. 1995; 34:14288–14292. [PubMed: 7578031]

Grönberg L, Ruan Z, Bittman R, Slotte JP. Biochemistry. 1991; 30:10746–10754. [PubMed: 1931994]

Hanada K, Nishijima M, Akamatsu Y, Pagano RE. J Biol Chem. 1995; 270:6254–6260. [PubMed: 7890763]

Harris JS, Epps DE, Davio SR, Kézdy FJ. Biochemistry. 1995; 34:3851–3857. [PubMed: 7893682]

Helm CA, Möhwald H, Kjaer K, Als-Nielsen J. Biophys J. 1987; 52:381–390. [PubMed: 3651557]

Helm CA, Tippmann-Krayer P, Möhwald H, Als-Nielsen J, Kjaer K. Biophys J. 1991; 60:1457–1476. [PubMed: 1777568]

Hwang J, Tamm LK, Böhm C, Ramalingam TS, Betzig E, Edidin M. Science. 1995; 270:610–614. [PubMed: 7570018]

Jarrell H, Singh D, Grant CWM. Biochim Biophys Acta. 1992; 1103:331–334. [PubMed: 1543718]

Johnston DS, Chapman D. Biochim Biophys Acta. 1988; 937:10–22. [PubMed: 3334840]

Koynova R, Caffrey MC. Biochim Biophys Acta. 1995; 1255:213–236. [PubMed: 7734437]

Kulkarni VS, Anderson WH, Brown RE. Biophys J. 1995; 69:1976–1986. [PubMed: 8580341]

Lund-Katz S, Laboda HM, McLean LR, Phillips MC. Biochemistry. 1988; 27:3416–3423. [PubMed: 3390441]

McIntosh TJ, Magid AD, Simon SA. Biochemistry. 1989; 28:17–25. [PubMed: 2706242]

McIntosh TJ, Simon SA, Needham D, Huang CC. Biochemistry. 1992a; 31:2012–2020. [PubMed: 1536844]

McIntosh TJ, Simon SA, Needham D, Huang CC. Biochemistry. 1992b; 31:2020–2024. [PubMed: 1536845]

Morrow MR, Singh D, Lu D, Grant CWM. Biophys J. 1995; 68:179–186. [PubMed: 7711240]

Murata M, Peränen J, Schreiner R, Wieland F, Kurzchalia TV, Simons K. Proc Natl Acad Sci USA. 1995; 92:10339–10343. [PubMed: 7479780]

Nieva JL, Bron R, Corver J, Wilschut J. EMBO J. 1994; 13:2797–2804. [PubMed: 8026464]

Oldfield E, Meadows M, Rice D, Jacobs R. Biochemistry. 1978; 17:2727–2740. [PubMed: 687560]

Palestini P, Allietta M, Sonnino S, Tettamanti G, Thompson TE, Tillack TW. Biochim Biophys Acta. 1995; 1235:221–230. [PubMed: 7756329]

Parton RG. J Histochem Cytochem. 1994; 42:155–166. [PubMed: 8288861]

Parton RG, Simons K. Science. 1995; 269:1398–1399. [PubMed: 7660120]

Phillips, MC. Progress in Surface and Membrane Science. Danielli, JF.; Rosenberg, MD.; Cadenhead, DA., editors. Vol. 5. Academic Press; New York: 1972. p. 139-221.

Phillips MC, Chapman D. Biochim Biophys Acta. 1968; 163:301–313. [PubMed: 5721894]

Robinson AJ, Richards WG, Thomas PJ, Hann MM. Biophys J. 1995; 68:164–170. [PubMed: 7711238]

Ruocco MJ, Shipley GG. Biochim Biophys Acta. 1983; 735:305–308. [PubMed: 6626552]

Sankaram MB, Thompson TE. Proc Natl Acad Sci USA. 1991; 88:8686–8690. [PubMed: 1656453]

Schroeder R, London E, Brown D. Proc Natl Acad Sci USA. 1994; 91:12130–12134. [PubMed: 7991596]

Sen A, Hui SW. Chem Phys Lipids. 1988; 49:179–184. [PubMed: 3240563]

Slotte JP. Biochim Biophys Acta. 1995; 1235:419–427. [PubMed: 7756352]

Slotte JP, Östman AL, Kumar ER, Bittman R. Biochemistry. 1993; 32:7886–7892. [PubMed: 8347594]

Smaby JM, Brockman HL. Biophys J. 1990; 58:195–204. [PubMed: 2383632]

Smaby JM, Brockman HL. Chem Phys Lipids. 1991; 58:249–252. [PubMed: 1893502]

Smaby JM, Brockman HL, Brown RE. Biochemistry. 1994; 33:9135–9142. [PubMed: 8049216]

Smaby JM, Kulkarni VS, Momsen M, Brown RE. Biophys J. 1996; 60:868–877. [PubMed: 8789104]

Smart EJ, Ying YS, Conrad PA, Anderson RGW. J Cell Biol. 1994; 127:1185–1197. [PubMed: 7962084]

Speyer JB, Weber RT, Das Gupta SK, Griffin RG. Biochemistry. 1989; 28:9569–9574. [PubMed: 2611249]

Vaknin D, Kjaer K, Als-Nielsen J, Lösche M. Biophys J. 1991; 59:1325–1332. [PubMed: 19431794]

Vanderkooi G. Biophys J. 1994; 66:1457–1468. [PubMed: 8061195]

Wilschut J, Corver J, Nieva J, Bron R, Moesby L, Reddy KC, Bittman R. Mol Membr Biol. 1995; 12:143–149. [PubMed: 7767374]

Yeagle PL, Hutton WC, Huang CH, Martin RB. Proc Natl Acad Sci USA. 1975; 72:3477–3481. [PubMed: 1059134]

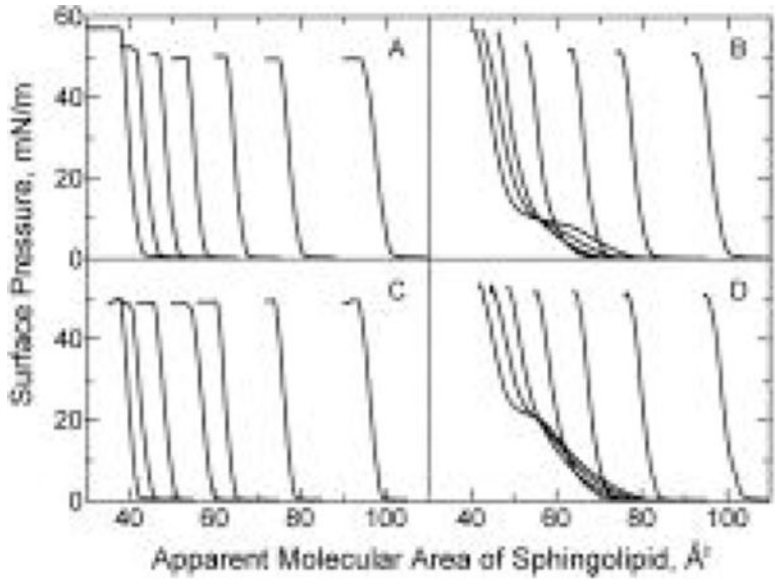

FIGURE 1.

Surface pressure vs apparent molecular area of sphingolipid. Isotherms were recorded at 24 °C on a subphase of 10 mM potassium phosphate (pH 6.6) containing 100 mM NaCl and 0.02% NaN_3. In each panel, cholesterol mole fractions increase by 0.1 in the isotherms such that X_{chol} = 0, 0.1, 0.2, 0.3, 0.4, 0.5, and 0.6 from left to right (at π = 30 mN/m): (A) 18:0 GalCer, (B) 18:0 SM, (C) 16:0 GalCer, and (D) 16:0 SM.

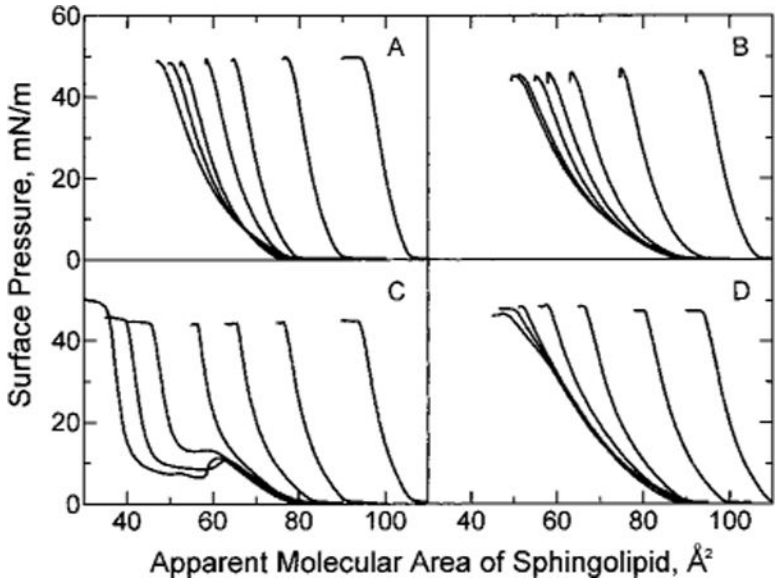

FIGURE 2.

Surface pressure vs apparent molecular area of sphingolipid. Experimental conditions were the same as in Figure 1: (A) 18:1 GalCer. (B) 18:1 SM, (C) 24:1 GalCer, and (D) 24:1 SM.

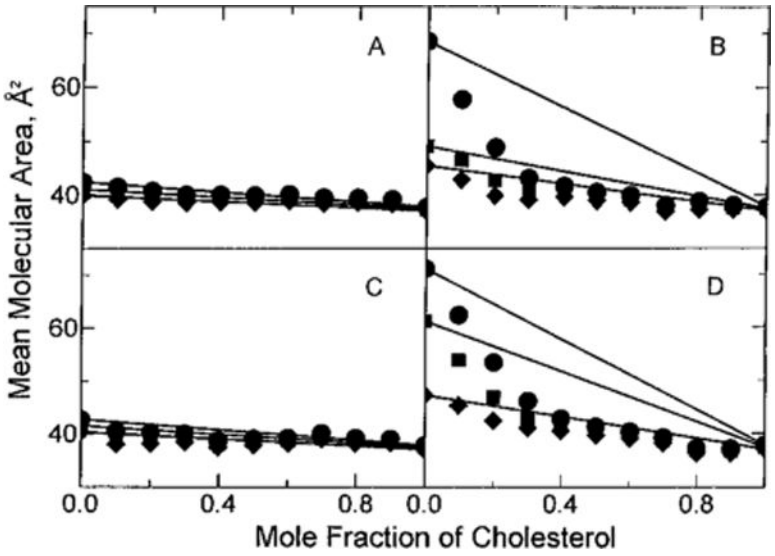

FIGURE 3.

Mean molecular area vs composition: (●) 5 mN/m, (■) 15 mN/m, and (◆) 30 mN/m. Experimental points are from the isotherms shown in Figure 1 and are indicated by the symbols. Solid lines represent ideal additivity of mean molecular area at the designated surface pressure and were calculated using eq 1 in Materials and Methods: (A) 18:0 GalCer, (B) 18:0 SM, (C) 16:0 GalCer, and (D) 16:0 SM.

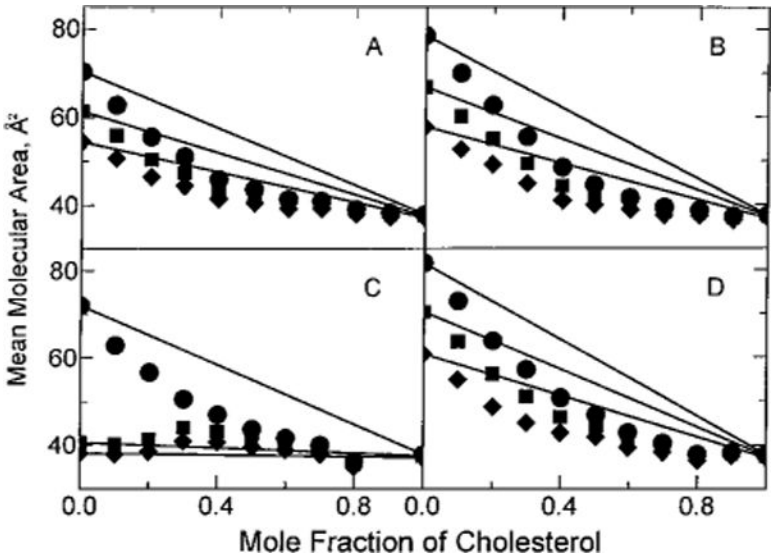

FIGURE 4.

Mean molecular area vs composition: (●) 5 mN/m, (■) 15 mN/m, and (◆) 30 mN/m. Experimental points are from the isotherms shown in Figure 2 and are indicated by the symbols. Solid lines represent ideal additivity of mean molecular area at the designated surface pressure and were calculated using eq 1 in Materials and Methods: (A) 18:1 GalCer, (B) 18:1 SM, (C) 24:1 GalCer, and (D) 24:1 SM.

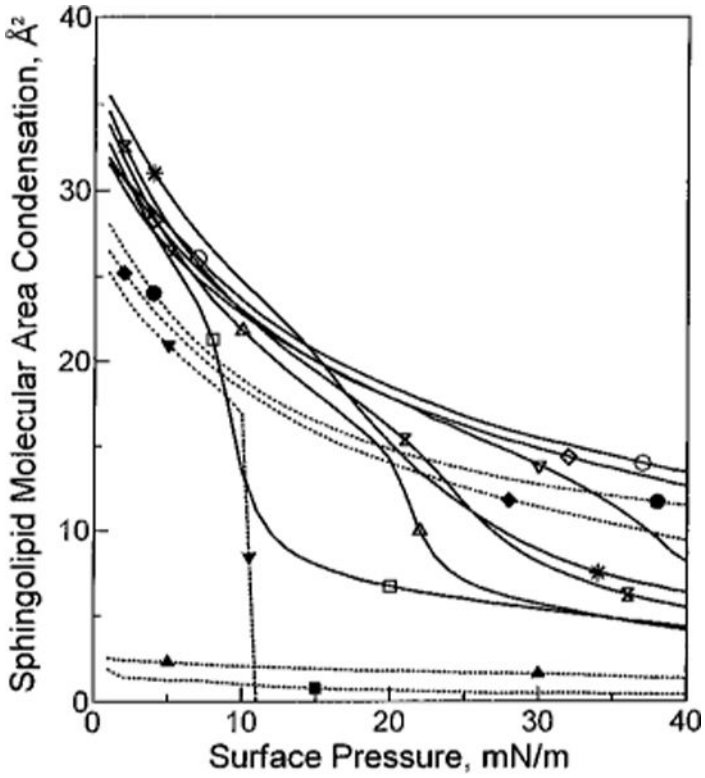

FIGURE 5.

Sphingolipid cross-sectional area condensation vs surface pressure. Each line represents the condensation observed when equimolar cholesterol is mixed with the designated sphingolipid at 24 °C. Solid lines represent different SMs. Dotted lines represent different GalCers. Area condensations were calculated as described in Materials and Methods. For each line, area condensation values were calculated at 1 mN/m intervals over the surface pressure range from 1 to 40 mN/m: (■) 18:0 GalCer, (▲) 16:0 GalCer, (▼) 24:1 GalCer, (□) 18:0 SM, (△) 16:0 SM, (bow tie) egg SM, (*) bovine SM, (◆) 18:1 GalCer, (●) 18:2 GalCer, (▽) 24:1 SM, (◇) 18:1 SM, and (○) 18:2 SM.

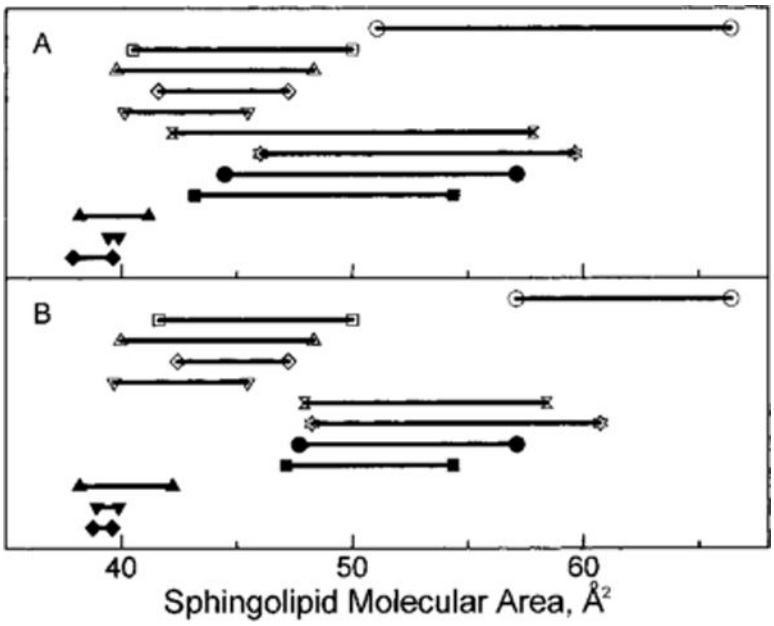

FIGURE 6.

Sphingolipid cross-sectional molecular area at 30 mN/m in the absence and presence of cholesterol. Each horizontal line corresponds to a different sphingolipid derivative (GalCers = filled symbols; SMs = unfilled symbols). The right-hand symbol represents the cross-sectional molecular area of the pure lipid in the absence of cholesterol; the left-hand symbol shows the condensed molecular area of each sphingolipid induced by either 0.5 (A) or 0.3 (B) mole fraction cholesterol. This latter area was calculated using eq 2 in Materials and Methods. The length of each horizontal line connecting paired symbols represents the change in sphingolipid molecular area, i.e. condensation, produced upon mixing with cholesterol: (○) 18:2 SM, (□) bovine SM, (△) egg SM, (◇) 16:0 SM, (▽) 18:0 SM, (bow tie) 18:1 SM, (☆) 24:1 SM, (●) 18:2 GalCer, (■) 18:1 GalCer, (▲) 24:1 GalCer, (▼) 18:0 GalCer, and (◆) 16:0 GalCer.

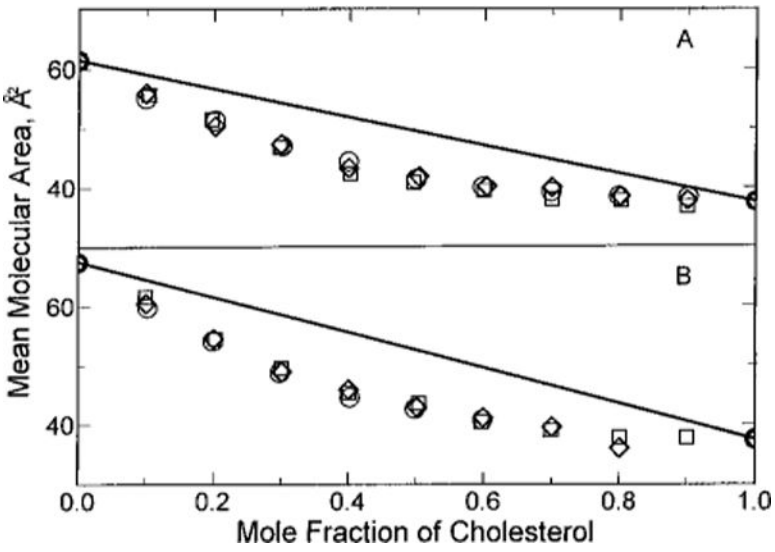

FIGURE 7.

Mean molecular area vs composition. First, the surface pressure necessary to achieve identical molecular areas in the liquid-expanded state was determined for each pure lipid. Then, the effect of cholesterol on the mean molecular areas of the mixed films was compared at each pure lipid's "area-equivalent" surface pressure. Ideal additivity is shown by the solid lines which were calculated using eq 1 in Materials and Methods. Experimental points are indicated by the symbols: (A) (○) 16:0, 18:1 PC at 30 mN/m, (□) 18:1 SM at 22.8 mN/m, and (◇) 18:1 GalCer at 14.75 mN/m; (B) (○) 16:0, 24:1 PC at 21.9 mN/m, (□) 24:1 SM at 18.1 mN/m, and (◇) 24:1 GalCer at 7 mN/m.